Description of the Global Mars Multiscale Model

Youssef Moudden, John C. McConnell
Department of Earth and Space Science and Engineering, York University, Toronto, Canada

This presentation describes a new three dimensional model for the Martian atmosphere. The dynamical core of the model, that deals with numerically solving the Navier-Stokes equations, has been adapted from the operational weather forecast model used in the Meteorological Service of Canada. The adapted grid-point dynamical core allows the definition of a region of variable horizontal resolution using a zooming system and hence the ability to conduct mesoscale simulations over areas of interest. Such mesoscale studies are usually performed using limited area models. The time resolution method is semi-implicit and the advection scheme is semi- Lagrangian, both characteristics allow moderate time steps to be used and high resolutions to be specified without affecting the stability of the model. The model uses the topography measured by the Mars Orbiter Laser Altimeter and the surface radiative properties measured by the Thermal Emission Spectrometer, both instruments are aboard the Mars Global Surveyor spacecraft launched to Mars in 1996. The model's vertical extent covers the atmosphere from the surface to 160-180 km. A new comprehensive radiative scheme has been developed and appended to the model to calculate the heating and cooling tendencies that result from Solar radiation and infra-red emission. The surface response to the radiative energy is obtained using a force-restore method. The convective activity in the turbulent boundary layer affects the large scale flow and an eddy diffusion parameterization gives the subgrid turbulent fluxes. Molecular diffusion becomes an important process in the low densities of the thermosphere, and thus thermal diffusion is included in the energy equation.

Below are some selected simulations of the models representing the surface temperatures and the boundary layer. Other results from the model are published in *Moudden and McConnell* (2005) and *Moudden et al.* (2005). Figure 1 is a direct comparison of the simulated surface temperatures with TES observations, 1(a) and 1(b) are an average of the simulated temperatures during 1 sol respectively in the low and high dust cases (optical depth 0.3 and 3), plots (c) and (d) are averages of measured surface temperatures by TES during 20 sol near southern summer solstice, the two plots are from two consecutive Martian years. Although the dust of the simulation does not match exactly the dust in the observed cases the agreement between 1(a) and 1(c)-(d) is quite good. The horizontal variability in the simulations is lower than in the observations. Since the surface response is being predominantly forced by the radiative fluxes, these results indicate that the main radiative processes are well represented by the heating scheme.Figure 2 shows surface temperature (a) and profiles of temperature (b), potential temperature (c) wind speed (d) and direction (e) and vertical velocity (f). The location is at 25°N and L_s=90°. the surface temperature (a) has a large diurnal range, approximately 95°K. The maximum temperature is about 260°K. The boundary layer is mainly driven by the diurnal oscillation of surface temperature and the plots of temperature and potential temperature (b and c) show a mixed layer as deep as 5 kilometers. Although there are no direct measurements of the depth of the Martian boundary layer the consensus from other 1D and 3D numerical simulations is that it can be 2 to 10 km deep and that the turbulence activity is many times stronger on Mars than on Earth due to a shallow atmosphere and a smaller gravity. At other latitudes (not shown here) the depth of the BL decreases gradually as we move away from the 25°N circle.

Figures 3 and 4 represents a mesoscale simulation using a non uniform grid.The model is used in its non-hydrostatic configuration and the horizontal grid is specified in a way that increases the resolution near the Viking lander 1 (VL1) site following the variable grid specification system. Figure 3b shows the grid used in this experiment which has an increased uniform resolution of 20 km centered around VL1 site over an area of 1000 km by 1200 km. Figure 3a shows the topography of the model in this simulation which is an interpolation of the high resolution MOLA topography to the specified grid. The time-step is kept at 1/25 sol. Figure 4 shows the temperatures and wind directions in synoptic views for three times during the day; at local noon at VL1 and approximately 5 hours before and after. The maximum surface temperature in figure 4b occurs near the Viking position since the planet's inclination ($\sim$24.9°) is close to the latitude of the lander ($\sim$22.5°) and planet's position in its orbit is near the solstice. The overall examination of the wind direction in the three Figures 4d, 4e and 4f shows the influence of the nearby topography in defining the observed daily rotation. The lander itself is located in relatively flat terrain but not far to the southwest direction is an important slope that directs the mainly south-north flow shown in Figure 4d in the northeast direction. As the Sun moves overhead (Fig 4e) the flow originates more from the southeast because the mouth of Valles Marineris located southeast of VL1 (see Figure 3) acts as a wind channel and the circulation follows the edge of the slope and gives a clockwise rotation inside the low terrain of Chryse Planitia. This configuration generates south or south-southeast winds at VL1 position. The flow turns northeast in Figure 4f and undergoes a clockwise rotation within Chryse Planitia and emerges with a south direction north of VL1. This situation produces east or east-northeast winds at VL1 at the end of the day and early evening. (See *Moudden et al.* (2005) for more discussion and comparison results.)

The evaluation of the model in its current state has revealed that it is a promising tool both in the uniform and zoomed configurations. The surface temperatures show the expected behavior regarding the diurnal variation and the changes related to the season and dust amount. The boundary layer profiles reflect the known features of the Martian boundary layer and the vertical profiles of temperature give a proper thermal structure. The zonal averages show a reasonable global meridional circulation and a good agreement with simulations from other models, especially in the mass streamfunction values that reflect the Hadley circulation. The agreement with the Thermal Emission Spectrometer temperature profiles is also encouraging. An important asset of this model is its ability to perform high resolution simulations over a limited area while remaining a global model. Selected simulations will be presented to illustrate this feature.

Acknowledgements: The authors wish to thank NSERC for continuing support.

References

Moudden, Y., and J. C. McConnell, A New Model for Multiscale Modeling of the Martian Atmosphere, GM3, *J. Geophys. Res., 110* doi:10.1029/2004JE002354, 2005.

Moudden, Y., J. C. McConnell, S. R. Beagley, M. A. Lopez-Valverde, M. A. Lopez-Puertas, Meteorological results From the Global Mars Multiscale Model at the Viking 1 Lander site, *Adv. Space Res.,* Volume 36, Issue 11, Pages 2169-2175, 2005.

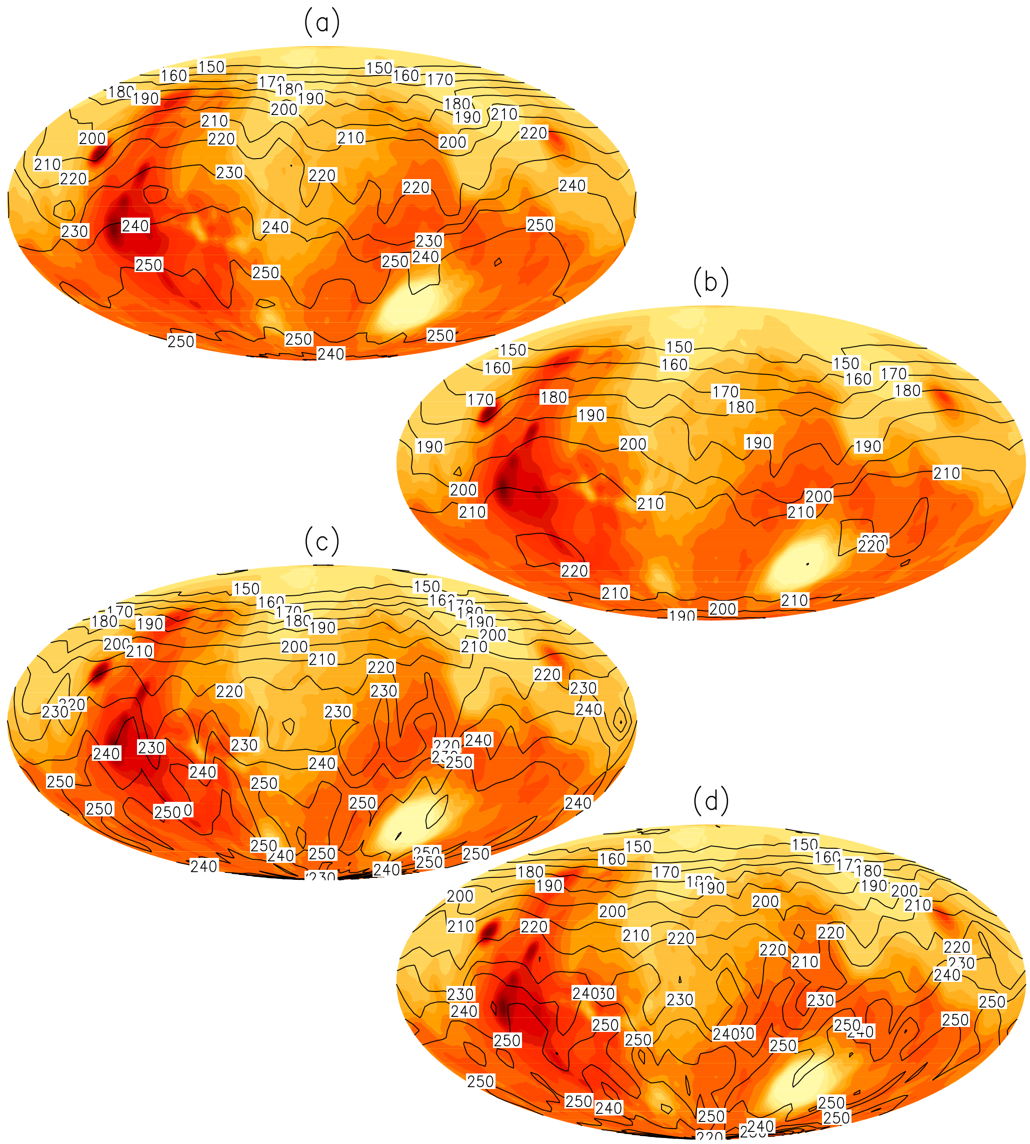

Figure 1: Comparison of the model's simulated diurnal average surface temperature in the low (a) and high (b) dust opacity cases, with the two years available observations from TES (c and d). The simulations are an average of 1 sol and the observations are an average of 20 sols near the southern summer solstice ($L_s = 270°$).

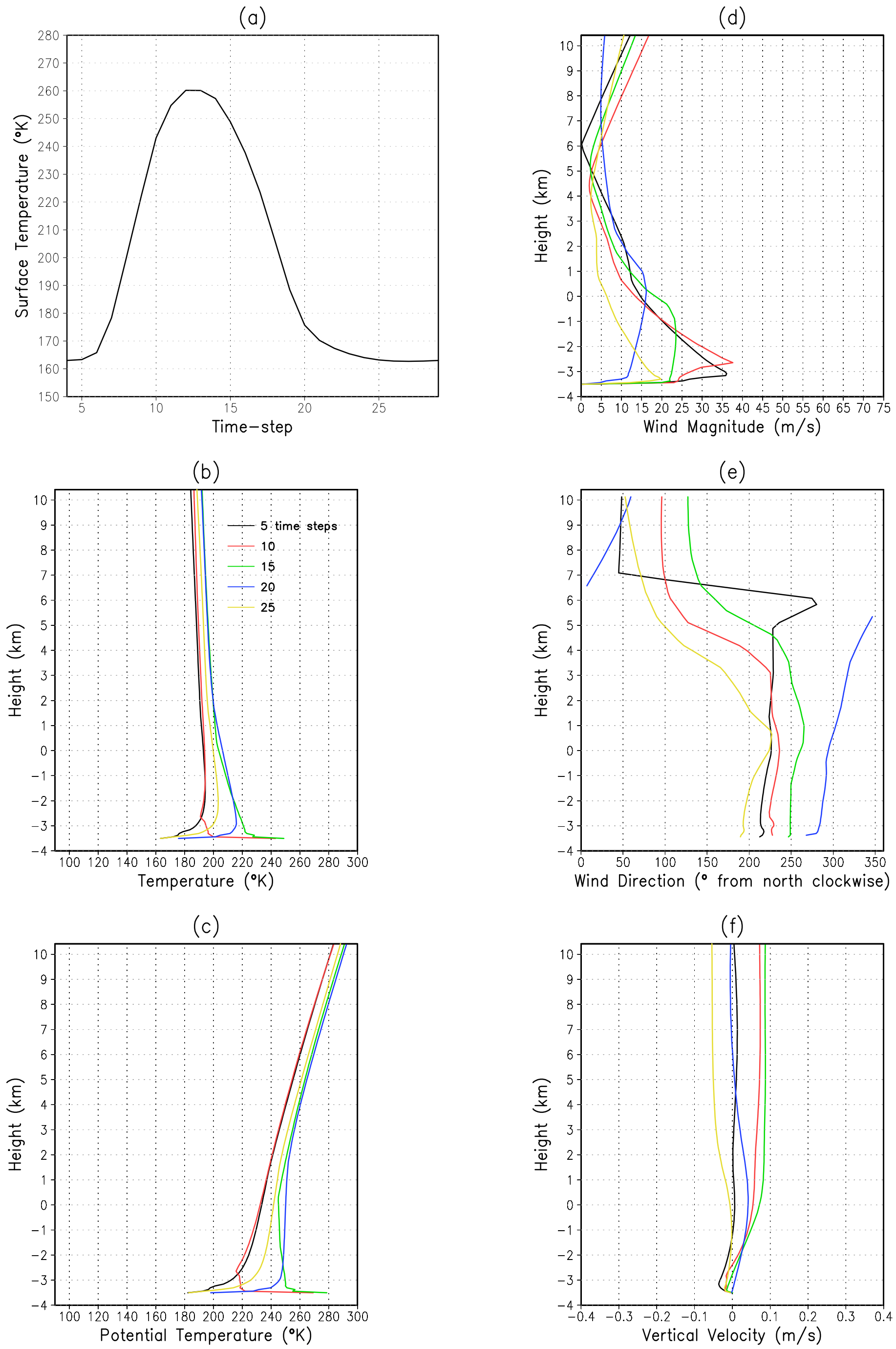

Figure 2: Boundary layer profiles as simulated for 1 sol in the northern summer solstice with an opacity of 0.5. The panels are (a) surface temperature, (b) atmosphere temperature, (c) potential temperature, (d) wind speed, (e) wind direction and (f) vertical velocity. The profiles are shown for every 5 time-steps.

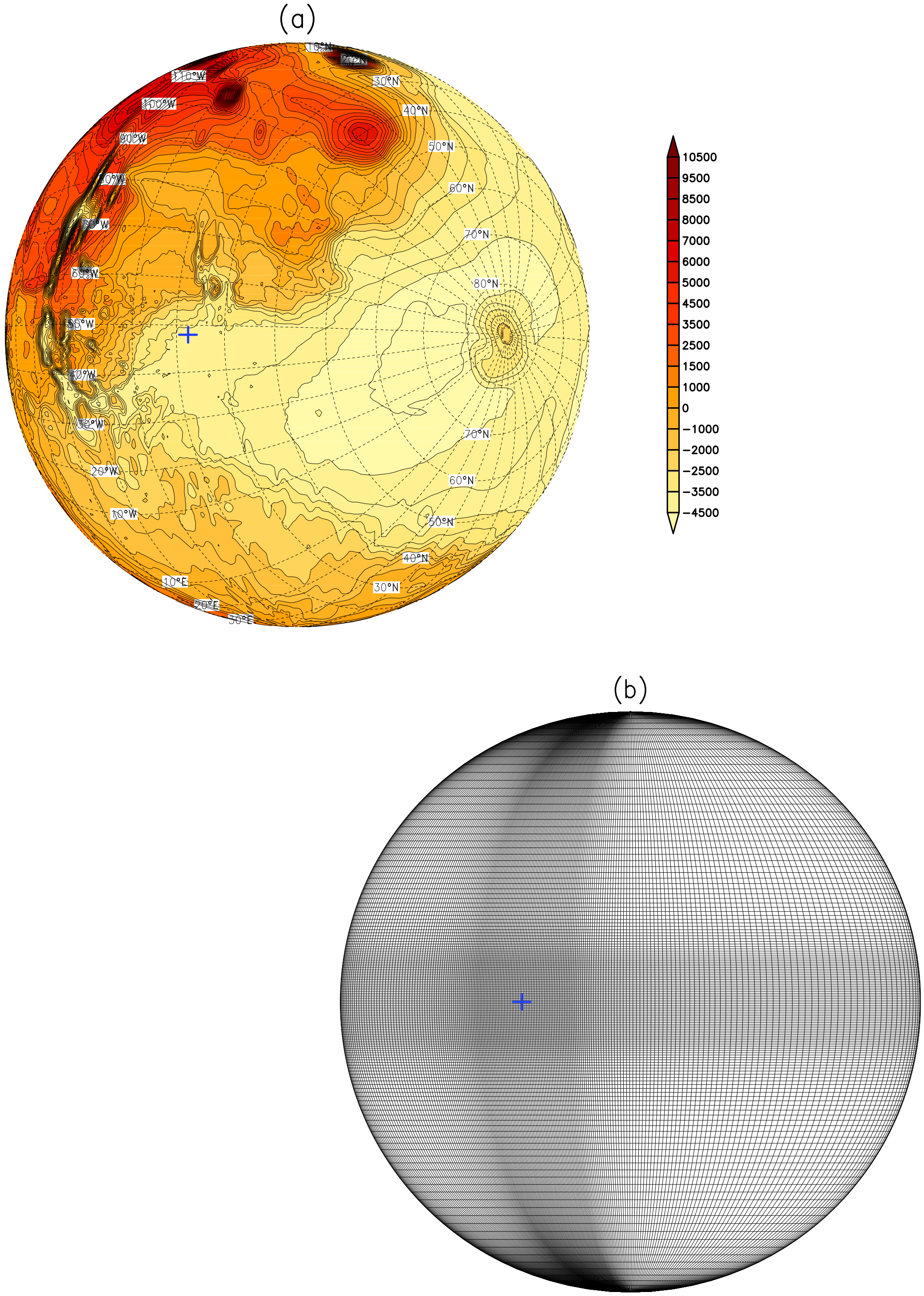

Figure 3: The model's topography (a) and variable resolution grid (b) in an orthographic projection. The cross indicates the position of Viking lander 1.

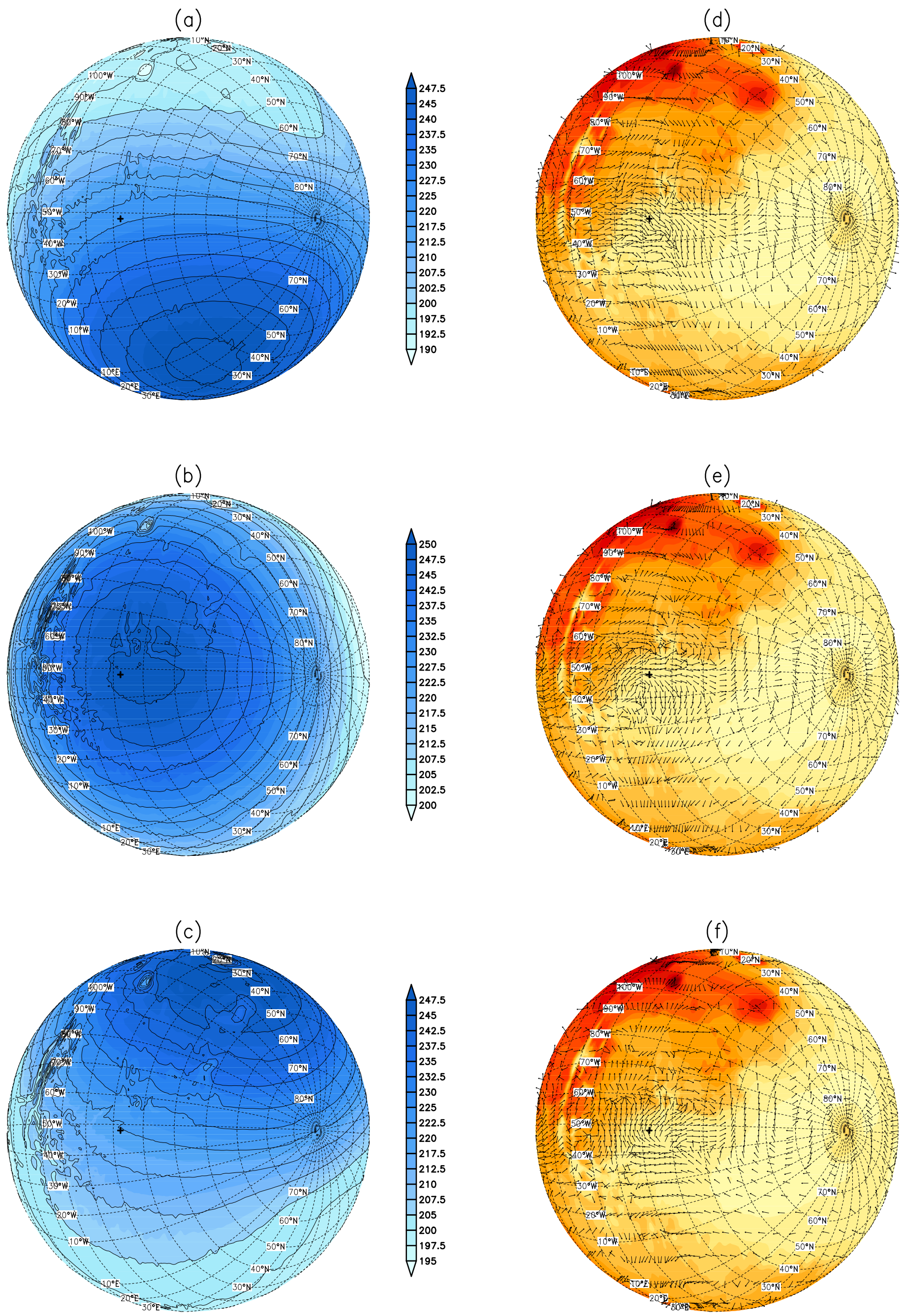

Figure 4: Surface temperatures (a, b and c) and first level wind direction (d, e and f) at 5 time steps interval in orthographic projections. The simulation is performed near the northern summer solstice ($L_s \sim 98$).